Statistical models for the analysis of BOLD and ASL Magnetic Resonance modalities

Aina Frau-Pascual

Advisors: Florence Forbes, Philippe Ciuciu

December 19th, 2016

Outline

Outline

Introduction to fMRI, BOLD and ASL

ASL fMRI data analysis

The ASL Joint Detection-Estimation framework

Contributions

Conclusions, perspectives and outcomes

Functional Magnetic Resonance Imaging

MRI scanner

Experimental design

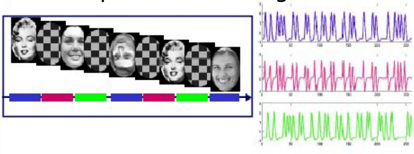

Functional Magnetic Resonance Imaging

MRI scanner

Experimental design

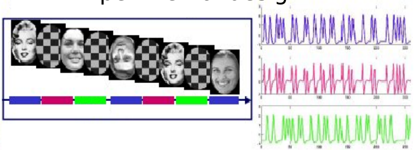

Neural activations

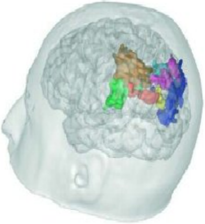

Functional Magnetic Resonance Imaging

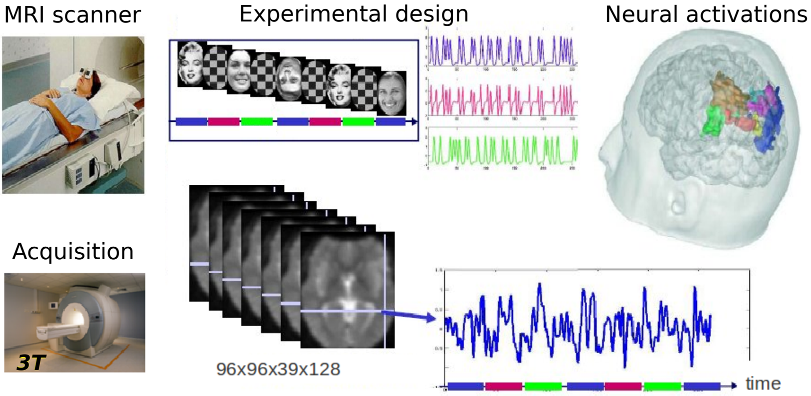

BOLD effect functional MRI

- Blood Oxygen Level Dependent [Ogawa et al, PNAS 1990]

What does BOLD contrast really measure?

BOLD measures the ratio of oxy- to deoxy-hemoglobin in the blood

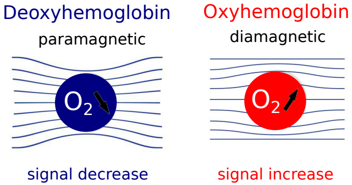

BOLD effect functional MRI

- Blood Oxygen Level Dependent [Ogawa et al, PNAS 1990]

What does BOLD contrast really measure?

BOLD measures the ratio of oxy- to deoxy-hemoglobin in the blood

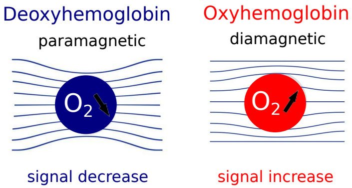

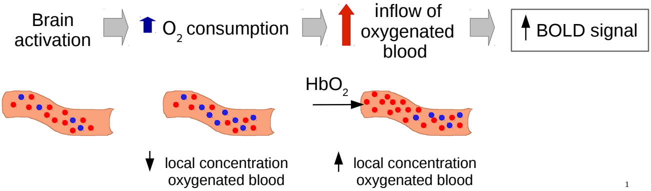

1

BOLD effect functional MRI

- Blood Oxygen Level Dependent [Ogawa et al, PNAS 1990]

What does BOLD contrast really measure?

BOLD measures the ratio of oxy- to deoxy-hemoglobin in the blood

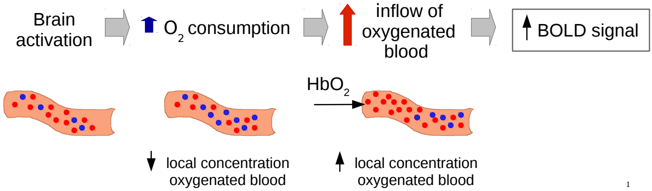

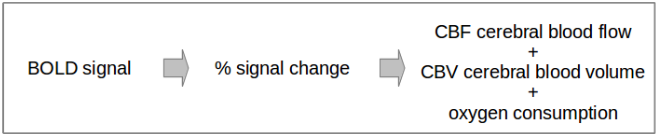

BOLD effect functional MRI

- Blood Oxygen Level Dependent [Ogawa et al, PNAS 1990]

What does BOLD contrast really measure?

BOLD measures the ratio of oxy- to deoxy-hemoglobin in the blood

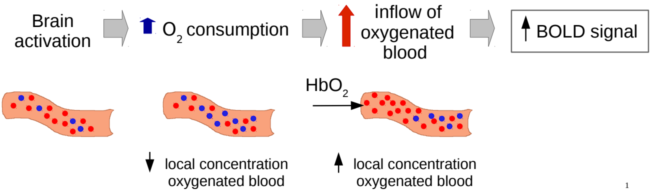

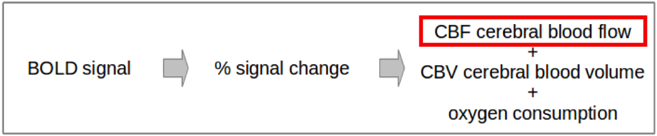

Quantitative measure of Cerebral Blood Flow

Cerebral perfusion or blood flow:
Delivery of nutritive blood to the brain tissue capillary bed

Absolute measure:

- More precise and direct
- **Perfusion altered in various diseases**
  [Cantin et al, 2011; Hamzei et al, 2003; Krainik et at, 2005]

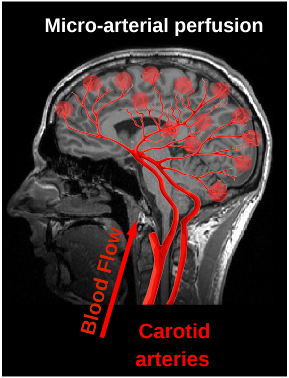

Brain image by T. Vincent

Arterial Spin Labelling data acquisition

- Arterial Spin Labelling [Williams et al, PNAS 1992]

Tag image

Tag inflowing arterial blood by magnetic inversion.

Control image

Repeat experiment without labelling inflowing blood.

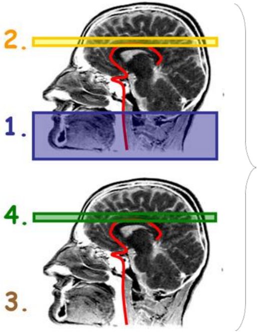

Control Image (4) - Tag Image (2)

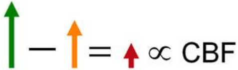

Ref: http://fmri.research.umich.edu/research/main_topics/asl.php

Arterial Spin Labelling data acquisition

- Arterial Spin Labelling [Williams et al, PNAS 1992]

Tag image

Tag inflowing arterial blood by magnetic inversion.

Control image

Repeat experiment without labelling inflowing blood.

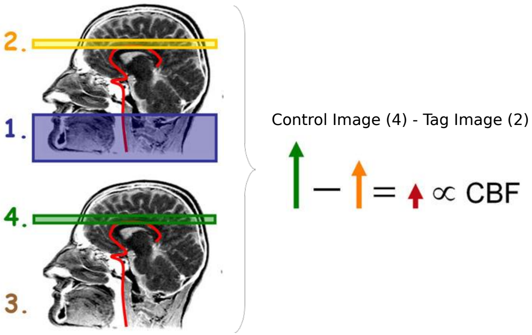

ASL contains also a hemodynamic or BOLD component!

Ref: http://fmri.research.umich.edu/research/main_topics/asl.php

Arterial Spin Labelling data acquisition: Tag image

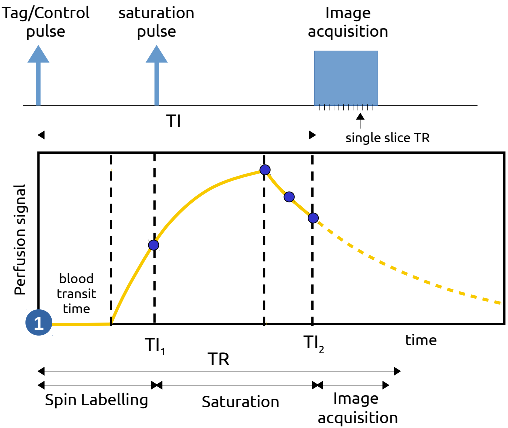

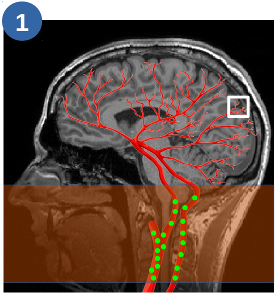

Brain images by T. Vincent

Arterial Spin Labelling data acquisition: Tag image

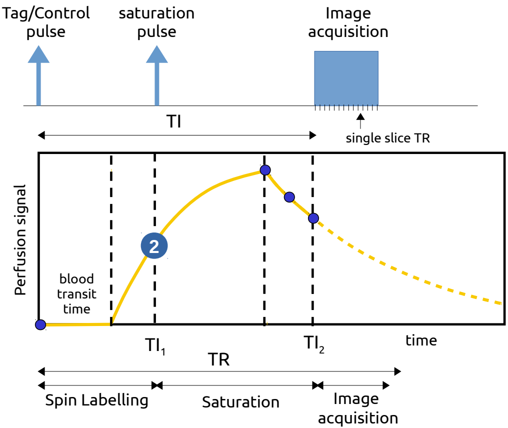

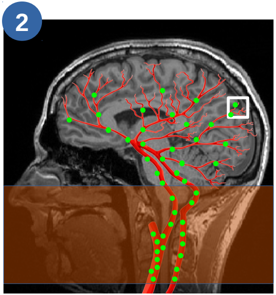

Brain images by T. Vincent

Arterial Spin Labelling data acquisition: Tag image

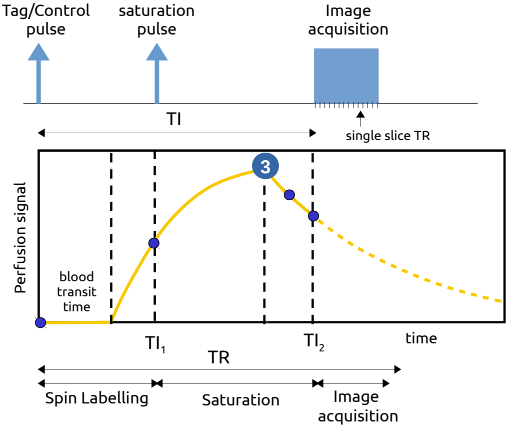

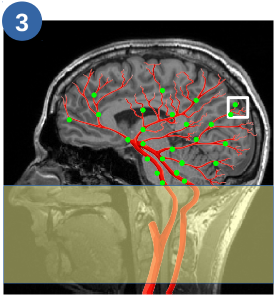

Brain images by T. Vincent

Arterial Spin Labelling data acquisition: Tag image

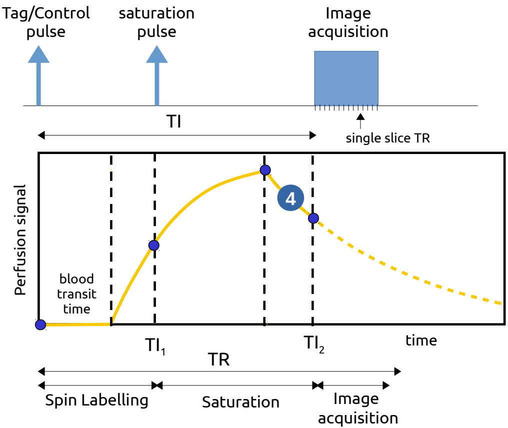

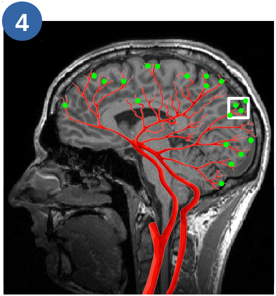

Brain images by T. Vincent

Arterial Spin Labelling data acquisition: Tag image

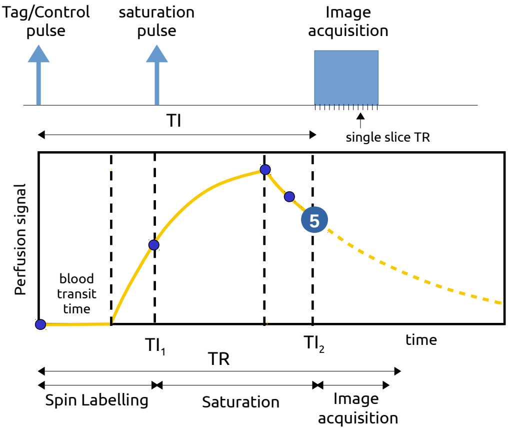

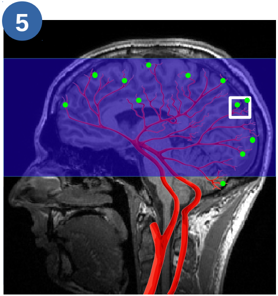

Brain images by T. Vincent

Arterial Spin Labelling quantification

CBF quantification can be achieved by applying a transformation [Buxton et al., 1998; Alsop et al., 2015].

$$CBF[mL/100g/min] = a \, \frac{M_{control} - M_{tag}}{M_0}$$

where

- $M_{control} - M_{tag}$: perfusion signal
- M_0: relaxed magnetization
- a: scale factor that considers acquisition parameters and blood transit

ASL vs BOLD imaging techniques

ASL	BOLD
✓ non invasive, non ionizing	✓ non invasive, non ionizing
✓ absolute measure	✗ relative measure
✓ cerebral blood flow	✗ mix of parameters
✗ low SNR ($\sim 1\%$ variation)	✓ higher SNR ($\sim 3-4\%$ variation)
✗ low resolution	✓ higher resolution
✓ highly reproducible	
✓ low inter-session variability	
✓ localized detection of activity	

Comparison: [Liu and Brown, 2007; Detre and Wang, 2002; Tjandra et al, 2005; Leontiev and Buxton, 2007; Raoult et al, 2011; Pimentel et al, 2013]

ASL applications

Clinical applications: Stroke, dementia, Alzheimers, Schizophrenia, Multiple Sclerosis, neuro-oncology.

[Wang, 2012; Wolk, 2012; Detre et al, 2012; Kindler, 2013; D'haeseller, 2013; Bron, 2014; Grade, 2015]

i2bm.cea.fr

Cognitive neuroscience

[Demeter et al, 2011; Buschkuehl et al, 2014]

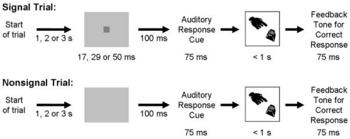

Drug studies

[Chen et al, 2011; Detre et al, 2012]

Photo credit: Tom Varco

Suitable for pediatric populations

[Wang et al, 2003; Detre et al, 2012]

unicog.org

This thesis is about...

Investigation of statistical models for the analysis of ASL and BOLD fMRI modalities.

ASL has a **high potential** but it is not widely used

Outline

ASL fMRI data

ASL data contain both hemodynamic and perfusion task-related components

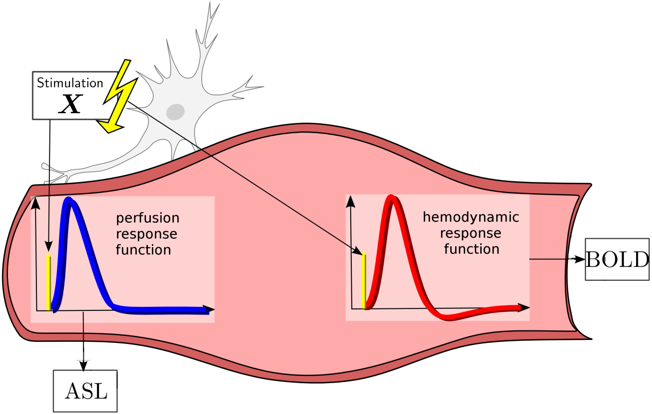

CBF

CBF + blood volume
+ oxygen consumption

ASL signal model: task-related components

ASL signal = task-related perfusion + task-related hemodyn.

$$\boldsymbol{y}_j = \sum_{m=1}^{M} \left(c_j^m \boldsymbol{W} \boldsymbol{X}^m \boldsymbol{g} + a_j^m \boldsymbol{X}^m \boldsymbol{h} \right)$$

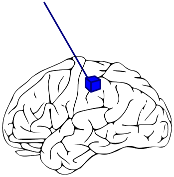

voxel

$\boldsymbol{g}$ 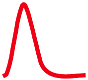

perfusion response function (PRF)

$\boldsymbol{h}$ 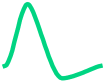

hemodynamic response function (HRF)

experimental condition

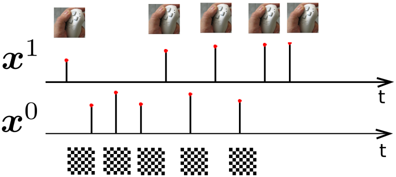

ASL signal model: task-related BOLD regressor

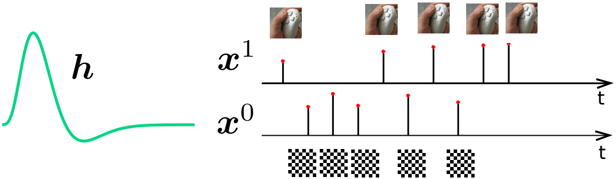

Assumptions:

linearity
stationarity
additivity

$(\boldsymbol{x}^0 * \boldsymbol{h})(t)$

$(\boldsymbol{x}^1 * \boldsymbol{h})(t)$

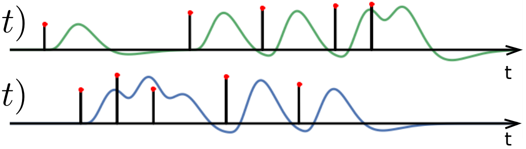

$(\boldsymbol{x}^0 * \boldsymbol{h})(t) + (\boldsymbol{x}^1 * \boldsymbol{h})(t)$

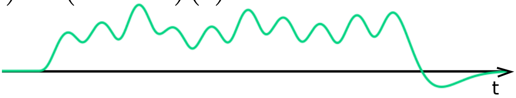

ASL signal model: task-related perfusion regressor

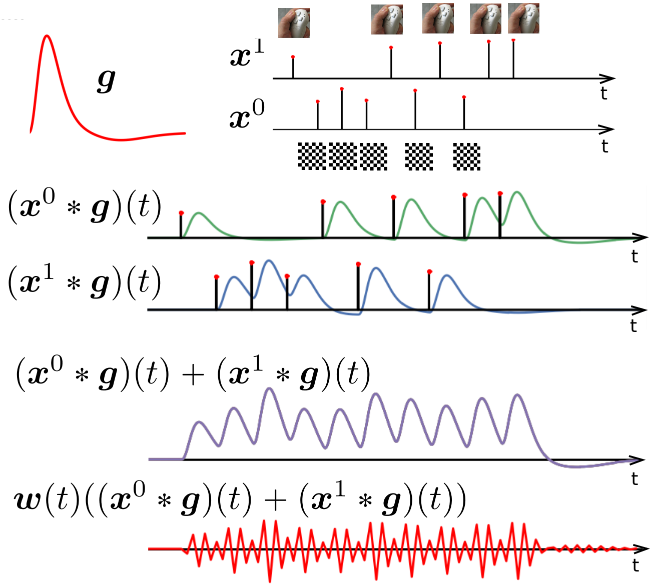

ASL signal model: task-related activation levels

ASL signal = task-related perfusion + task-related hemodyn.

$$\boldsymbol{y}_j = \sum_{m=1}^{M} \left(c_j^m \boldsymbol{W} \boldsymbol{X}^m \boldsymbol{g} + a_j^m \boldsymbol{X}^m \boldsymbol{h} \right)$$

$\boldsymbol{g}$

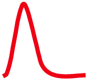

perfusion response function (PRF)

$\boldsymbol{h}$

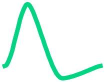

hemodynamic response function (HRF)

$\boldsymbol{c}$

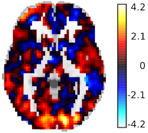

perfusion effect maps

$\boldsymbol{a}$

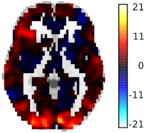

hemodynamic effect maps

ASL signal model: perfusion baseline

ASL signal = perfusion baseline + task-related perfusion + task-related hemodyn.

$$\boldsymbol{y}_j = \alpha_j \boldsymbol{w} + \sum_{m=1}^{M} \left(c_j^m \boldsymbol{W} \boldsymbol{X}^m \boldsymbol{g} + a_j^m \boldsymbol{X}^m \boldsymbol{h} \right)$$

$\boldsymbol{g}$

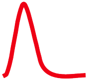

perfusion response function (PRF)

$\boldsymbol{h}$

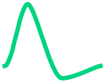

hemodynamic response function (HRF)

$\boldsymbol{\alpha}$

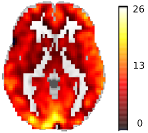

$\boldsymbol{c}$

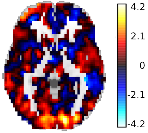

perfusion effect maps

$\boldsymbol{a}$

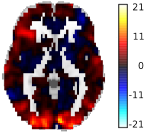

hemodynamic effect maps

ASL signal model: drifts and noise

$$\text{ASL signal} = \text{perfusion baseline} + \text{task-related perfusion} + \text{task-related hemodyn.} + \text{drift term} + \text{noise term}$$

$$\boldsymbol{y}_j = \alpha_j \boldsymbol{w} + \sum_{m=1}^{M} \left(c_j^m \boldsymbol{W} \boldsymbol{X}^m \boldsymbol{g} + a_j^m \boldsymbol{X}^m \boldsymbol{h} \right) + \boldsymbol{P}\boldsymbol{\ell}_j + \boldsymbol{b}_j$$

$\boldsymbol{g}$

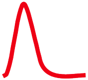

perfusion response function (PRF)

$\boldsymbol{h}$

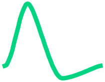

hemodynamic response function (HRF)

$\boldsymbol{\alpha}$

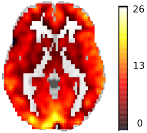

$\boldsymbol{c}$

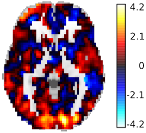

perfusion effect maps

$\boldsymbol{a}$

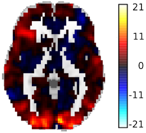

hemodynamic effect maps

ASL signal model: bilinear model

$$\boldsymbol{y}_j = \sum_{m=1}^{M} c_j^m \boldsymbol{W} \boldsymbol{X}^m \boldsymbol{g} + a_j^m \boldsymbol{X}^m \boldsymbol{h} + \alpha_j \boldsymbol{w} + \boldsymbol{P} \boldsymbol{\ell}_j + \boldsymbol{b}_j$$

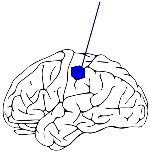

- Many unknowns
  $\phi = \{\boldsymbol{a}_j, \boldsymbol{h}, \boldsymbol{c}_j, \boldsymbol{g}, \boldsymbol{q}, \alpha_j, \boldsymbol{\ell}_j, \boldsymbol{b}_j\}$

- Bilinear model

Statistical analysis of ASL fMRI data

- General Linear Model (GLM)
  [Hernandez-Garcia et al, 2010; Mumford et al, 2006]

  Fixed response function shapes (HRF, PRF) $\boldsymbol{g}$ $\boldsymbol{h}$

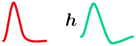

$$\boldsymbol{y}_j = \left(\boldsymbol{w}, \quad \boldsymbol{W}\boldsymbol{X}^m\boldsymbol{g}, \quad \boldsymbol{X}^m\boldsymbol{h}, \quad \boldsymbol{P} \right) \begin{pmatrix} \alpha_j \\ \boldsymbol{c}_j \\ \boldsymbol{a}_j \\ \boldsymbol{\ell}_j \end{pmatrix}$$

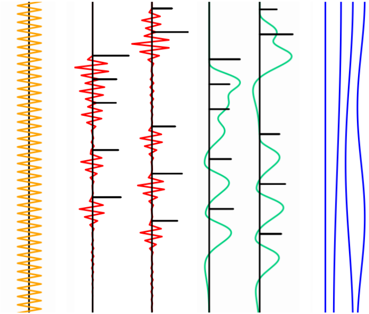

Inaccurate activation detection

Statistical analysis of ASL fMRI data

- Joint Detection-Estimation (JDE) [Vincent et al, 2013]

  Separate estimation of 2 response functions (HRF & PRF)
  A Bayesian framework allows to account for **prior knowledge on the parameters** $\phi = \{\boldsymbol{h}, \boldsymbol{g}, \boldsymbol{a}_j, \boldsymbol{c}_j, \alpha_j, \boldsymbol{\ell}_j, \boldsymbol{b}_j\}$
  Parcel-wise model

Implementation computationally expensive

PRF estimation not satisfactory

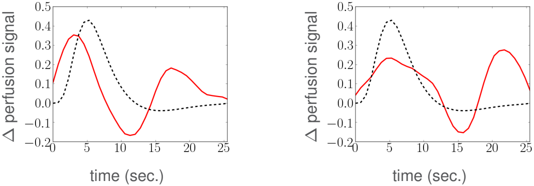

Outline

ASL Joint Detection-Estimation: a Bayesian framework

$$\underbrace{\boxed{p(\phi|y)}}_{\text{posterior}} = \frac{\overbrace{\boxed{p(y|\phi)}}^{\text{likelihood}}\ \overbrace{\boxed{p(\phi)}}^{\text{prior}}}{\underbrace{\boxed{p(y)}}_{\substack{\text{model evidence}\\ \text{marginal likelihood}}}}$$

$p(y) = \int_\phi p(y|\phi)p(\phi)d\phi$ is a normalizing constant, and it is often intractable.

ASL fMRI Bayesian analysis: likelihood

$$\underbrace{p(\phi|y)}_{\text{posterior}} = \frac{\boxed{\overbrace{p(y|\phi)}^{\text{likelihood}}}\ \overbrace{p(\phi)}^{\text{prior}}}{\underbrace{p(y)}_{\substack{\text{model evidence}\\ \text{marginal likelihood}}}}$$

The **likelihood** of our model reads

$$p(\boldsymbol{y}_j|\boldsymbol{\phi}) \sim \mathcal{N}\left(\sum_{m=1}^{M} c_j^m \boldsymbol{W}\boldsymbol{X}^m \boldsymbol{g} + a_j^m \boldsymbol{X}^m \boldsymbol{h} + \alpha_j \boldsymbol{w} + \boldsymbol{P}\boldsymbol{\ell}_j, v_b \boldsymbol{\Gamma}_j^{-1}\right)$$

where the variance comes from the noise $\boldsymbol{b}_j \sim \mathcal{N}(0, v_b \boldsymbol{\Gamma}_j^{-1})$ and $\phi = \{\boldsymbol{a}_j, \boldsymbol{h}, \boldsymbol{c}_j, \boldsymbol{g}, \boldsymbol{q}, \alpha_j, \boldsymbol{\ell}_j, \theta\}$

ASL fMRI Bayesian analysis: JDE priors

$$\underbrace{p(\phi|y)}_{\text{posterior}} = \frac{\overbrace{p(y|\phi)}^{\text{likelihood}}\;\boxed{\overbrace{p(\phi)}^{\text{prior}}}}{\underbrace{p(y)}_{\substack{\text{model evidence}\\ \text{marginal likelihood}}}}$$

In a given parcel:

Prior on the response functions to enforce temporal regularization:

$$\boldsymbol{h} \sim \mathcal{N}(0, v_h \boldsymbol{R})$$
$$\boldsymbol{g} \sim \mathcal{N}(0, v_g \boldsymbol{R})$$

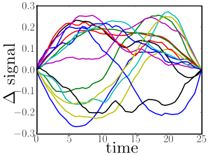

Priors on the response levels enforce spatial regularization:

$$\boldsymbol{a}_j|\boldsymbol{q}_j \text{ and } \boldsymbol{c}_j|\boldsymbol{q}_j$$

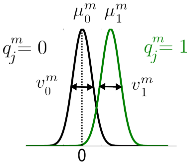

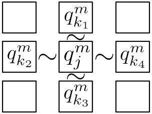

Prior on the perfusion baseline $\boldsymbol{\alpha}$ Gaussian: $\alpha_j \sim \mathcal{N}(0, v_\alpha \boldsymbol{I})$

ASL fMRI Bayesian analysis: JDE inference

$$\boxed{\underbrace{p(\phi|y)}_{\text{posterior}}} = \frac{\overbrace{p(y|\phi)}^{\text{likelihood}}\ \overbrace{p(\phi)}^{\text{prior}}}{\underbrace{p(y)}_{\substack{\text{model evidence}\\ \text{marginal likelihood}}}}$$

In our model, we have $\phi = \{a, h, c, g, q, \alpha, \ell, \theta\}$ and the posterior is intractable $\rightarrow$ need for **inference approximation**:

- Markov Chain Monte Carlo (MCMC)
- Variational Expectation-Maximization (VEM)

Outline

Outline

Introduction to fMRI, BOLD and ASL

ASL fMRI data analysis

The ASL Joint Detection-Estimation framework

Contributions

- Hemodynamically informed parcellation of BOLD fMRI
- Fast multiple-session extension of JDE for BOLD fMRI
- Physiological prior
- Physiological models comparison in the analysis of ASL
- Physiologically informed JDE ASL solutions
- Validation of the methods compared to classical ones

Conclusions, perspectives and outcomes

Outline

Physiological prior: Balloon model

[Buxton et al, 1998; Friston et al, 2000; Khalidov et al, 2011]

$$\begin{cases} \dfrac{df_{in}(t)}{dt} = \psi(t) \\ \dfrac{d\psi(t)}{dt} = \eta u(t) - \dfrac{\psi(t)}{\tau_\psi} - \dfrac{f_{in}(t)-1}{\tau_f} \end{cases}$$

$$\begin{cases} \dfrac{dq(t)}{dt} = \dfrac{1}{\tau_m}\left(f_{in}(t)\dfrac{1-(1-E_0)^{1/f_{in}(t)}}{E_0} - q(t)v(t)^{\frac{1}{w}-1}\right) \\ \dfrac{dv(t)}{dt} = \dfrac{1}{\tau_m}\left(f_{in}(t) - v(t)^{\frac{1}{w}}\right) \end{cases}$$

$$h(t) = V_0[k_1(1-q(t)) + k_2(1-\frac{q(t)}{v(t)}) + k_3(1-v(t))]$$

$$g(t) = f_{in}(t) - 1$$

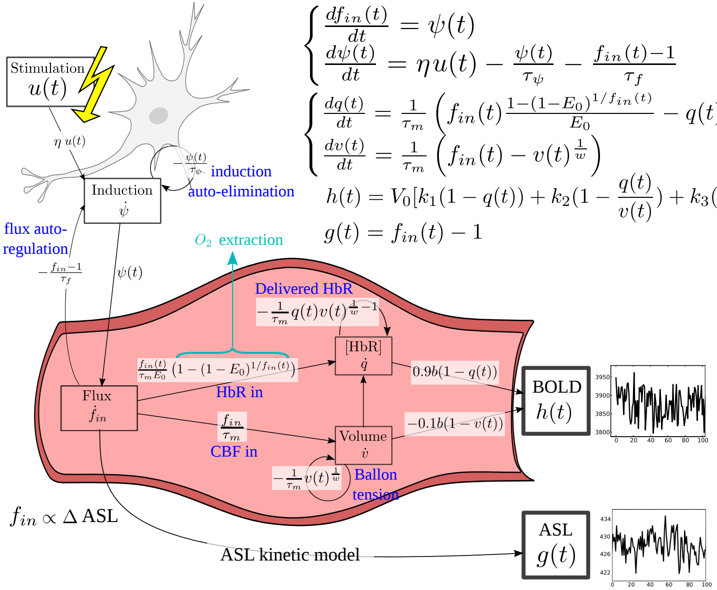

Physiological linear operator

[Buxton et al, 1998; Friston et al, 2000; Khalidov et al, 2011]

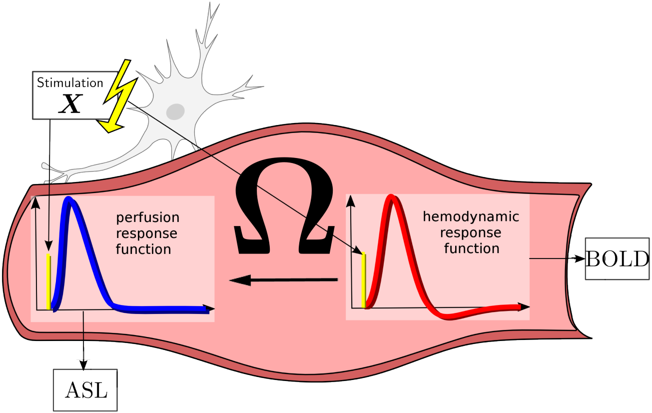

The linear operator Ω links perfusion and hemodynamic response functions: $g = \Omega h$

Physiological prior

How to incoporate the approximate link $g = \Omega h$?

- Conditional prior:

$$\boldsymbol{h} \sim \mathcal{N}(0, v_h \Sigma_h)$$
$$\boldsymbol{g}|\boldsymbol{h} \sim \mathcal{N}(\boldsymbol{\Omega h}, v_g \Sigma_g)$$

where Σ_g and Σ_h are chosen a priori.

HRF estimation remains the same and **the operator Ω couples the estimation of PRF to HRF**

Impact of the physiological prior

Paradigm: fast event-related design (mean ISI $= 5.1$s.), with 60 auditory and visual stimuli. AINSI dataset. Region on the **auditory cortex**.

JDE ASL (no physiological information) [Vincent et al, 2013]

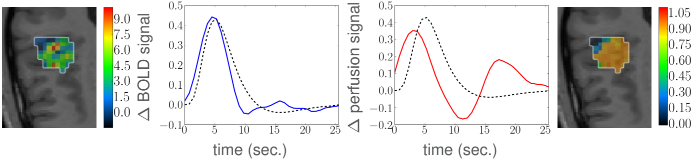

Physiologically informed JDE ASL [Frau-Pascual et al, 2014]

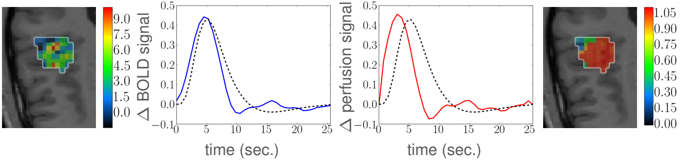

BRLs **BRF** **PRF** **PRLs**

The introduction of a physiological prior **improves PRF estimation**

Impact of the physiological prior

Paradigm: fast event-related design (mean ISI $= 5.1$s.), with 60 auditory and visual stimuli. AINSI dataset. Region on the **visual cortex**.

JDE ASL (no physiological information) [Vincent et al, 2013]

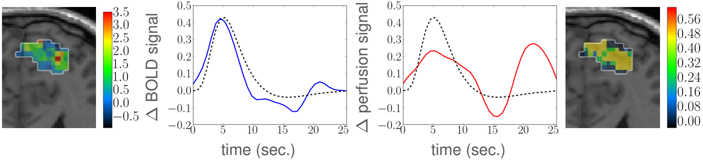

Physiologically informed JDE ASL [Frau-Pascual et al, 2014]

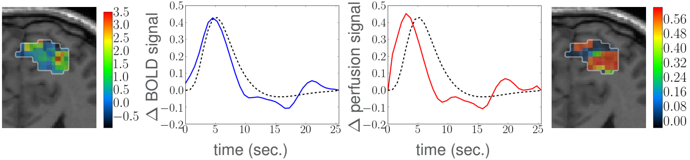

BRLs **BRF** **PRF** **PRLs**

The introduction of a physiological prior **improves PRF estimation**

Outline

Introduction to fMRI, BOLD and ASL

ASL fMRI data analysis

The ASL Joint Detection-Estimation framework

Contributions

- Hemodynamically informed parcellation of BOLD fMRI
- Fast multiple-session extension of JDE for BOLD fMRI
- Physiological prior
- Physiological models comparison in the analysis of ASL
- Physiologically informed JDE ASL solutions
- Validation of the methods compared to classical ones

Conclusions, perspectives and outcomes

Physiological models comparison: versions

Different versions of the extended Balloon model have been proposed in the literature [Stephan et al., 2007]:

$$\begin{cases} \frac{df_{in}(t)}{dt} = \psi(t) \\ \frac{d\psi(t)}{dt} = \eta u(t) - \frac{\psi(t)}{\tau_\psi} - \frac{f_{in}(t)-1}{\tau_f} \end{cases}$$

$$\begin{cases} \frac{dq(t)}{dt} = \frac{1}{\tau_m}\left(f_{in}(t)\frac{1-(1-E_0)^{1/f_{in}(t)}}{E_0} - q(t)v(t)^{\frac{1}{w}-1}\right) \\ \frac{dv(t)}{dt} = \frac{1}{\tau_m}\left(f_{in}(t) - v(t)^{\frac{1}{w}}\right) \end{cases}$$

$$\boxed{h(t) = V_0[k_1(1-q(t)) + k_2(1-\frac{q(t)}{v(t)}) + k_3(1-v(t))]}$$

$$g(t) = f_{in}(t) - 1$$

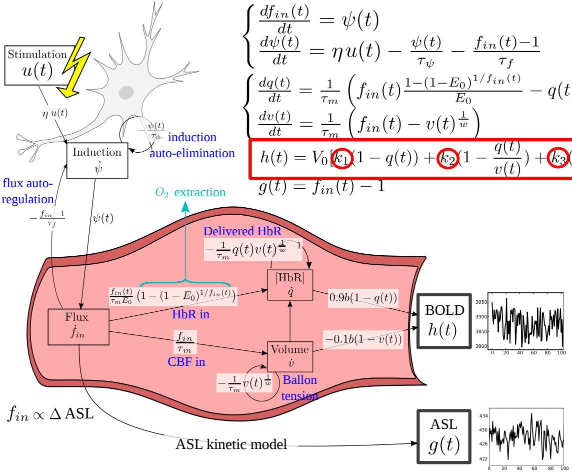

Physiological models comparison: parameters

Different physiological parameters have been also proposed [Friston et al, 2000; Khalidov et al, 2011].

$$\begin{cases} \frac{df_{in}(t)}{dt} = \psi(t) \\ \frac{d\psi(t)}{dt} = \eta u(t) - \frac{\psi(t)}{\tau_\psi} - \frac{f_{in}(t)-1}{\tau_f} \end{cases}$$

$$\begin{cases} \frac{dq(t)}{dt} = \frac{1}{\tau_m}\left(f_{in}(t)\frac{1-(1-E_0)^{1/f_{in}(t)}}{E_0} - q(t)v(t)^{\frac{1}{w}-1}\right) \\ \frac{dv(t)}{dt} = \frac{1}{\tau_m}\left(f_{in}(t) - v(t)^{\frac{1}{w}}\right) \end{cases}$$

$$h(t) = V_0[k_1(1-q(t)) + k_2(1-\frac{q(t)}{v(t)}) + k_3(1-v(t))]$$

$$g(t) = f_{in}(t) - 1$$

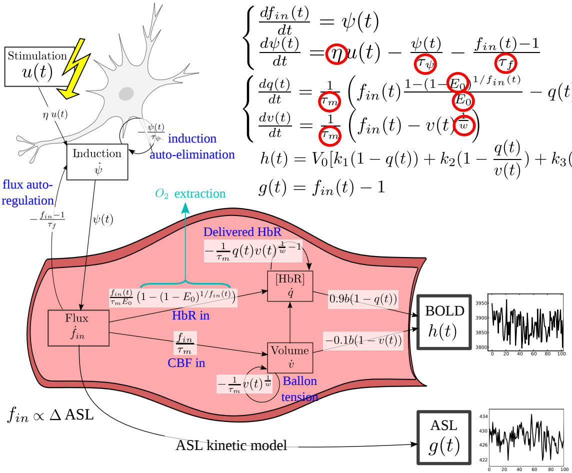

Physiological models comparison: parameters

Different physiological parameters have been also proposed [Friston et al, 2000; Khalidov et al, 2011].

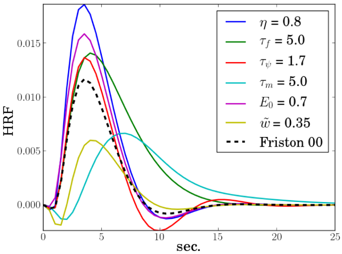

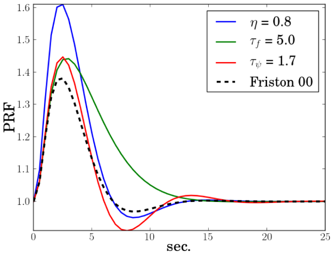

Sensitivity analysis of the physiological prior

[Frau-Pascual et al, 2015a]

Convergence of the average relative reconstruction error

$$e_{rec} = \frac{\|\boldsymbol{y}_{measured} - \boldsymbol{y}_{estim}\|^2}{\|\boldsymbol{y}_{measured}\|^2}$$

over 10 runs for the auditory cortex.

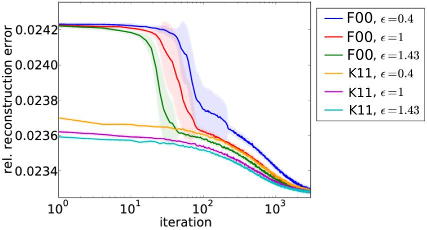

From experiments on 8 subject real data, we could conclude

- Parameter changes had more impact than model version.
- The best set of model/parameters causes a faster convergence: [Khalidov et al, 2011], $\epsilon = 1.43$

Outline

Introduction to fMRI, BOLD and ASL

ASL fMRI data analysis

The ASL Joint Detection-Estimation framework

Contributions

- Hemodynamically informed parcellation of BOLD fMRI
- Fast multiple-session extension of JDE for BOLD fMRI
- Physiological prior
- Physiological models comparison in the analysis of ASL
- Physiologically informed JDE ASL solutions
- Validation of the methods compared to classical ones

Conclusions, perspectives and outcomes

ASL JDE: methodology

$$\boxed{\underbrace{p(\phi|y)}_{\text{posterior}}} = \frac{\overbrace{p(y|\phi)}^{\text{likelihood}}\ \overbrace{p(\phi)}^{\text{prior}}}{\underbrace{p(y)}_{\substack{\text{model evidence}\\ \text{marginal likelihood}}}}$$

In our model, we have $\phi = \{a, h, c, g, q, \alpha, \ell, \theta\}$ and the posterior is intractable $\rightarrow$ need for **inference approximation**:

- Markov Chain Monte Carlo (MCMC)
- Variational Expectation-Maximization (VEM)

ASL JDE: Sampling with MCMC

[Vincent et al, 2013; Frau-Pascual et al, 2014]

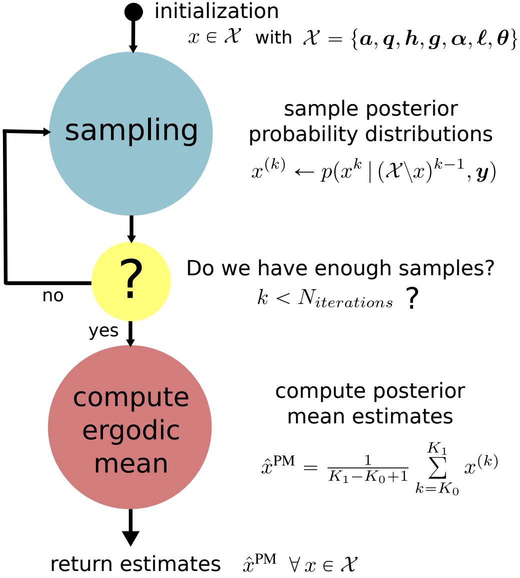

ASL JDE: Sampling with MCMC

[Vincent et al, 2013; Frau-Pascual et al, 2014]

MCMC is very **computationally expensive !!!**

ASL JDE: Approximate inference with VEM

Approximation of the posterior $p(\boldsymbol{a}, \boldsymbol{h}, \boldsymbol{c}, \boldsymbol{g}, \boldsymbol{q}|\boldsymbol{y})$ distribution with a computationally tractable expression, e.g. mean field:

$$\tilde{p}(\boldsymbol{a}, \boldsymbol{h}, \boldsymbol{c}, \boldsymbol{g}, \boldsymbol{q}) = \tilde{p}_a(\boldsymbol{a})\, \tilde{p}_h(\boldsymbol{h})\, \tilde{p}_c(\boldsymbol{c})\, \tilde{p}_g(\boldsymbol{g})\, \tilde{p}_q(\boldsymbol{q})$$

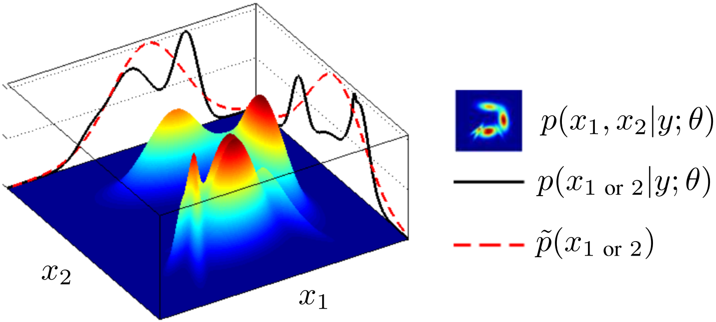

Jean Daunizeau https://sites.google.com/site/jeandaunizeauswebsite/

ASL JDE: Approximate inference with VEM

Expectation Maximization of a negative free energy function

$$\textbf{E-step: } \tilde{p}^{(r)} = \arg\max_{\tilde{p}} \; \mathcal{F}(\tilde{p}, y, \boldsymbol{\theta}^{(r)})$$

$$\textbf{M-step: } \boldsymbol{\theta}^{(r+1)} = \arg\max_{\boldsymbol{\theta}} \; \mathcal{F}(\tilde{p}^{(r)}, y, \boldsymbol{\theta})$$

ASL JDE: Approximate inference with VEM

Expectation Maximization of a negative free energy function

$$\textbf{E-step: } \tilde{p}^{(r)} = \arg\max_{\tilde{p}} \; \mathcal{F}(\tilde{p}, y, \boldsymbol{\theta}^{(r)})$$

$$\textbf{M-step: } \boldsymbol{\theta}^{(r+1)} = \arg\max_{\boldsymbol{\theta}} \; \mathcal{F}(\tilde{p}^{(r)}, y, \boldsymbol{\theta})$$

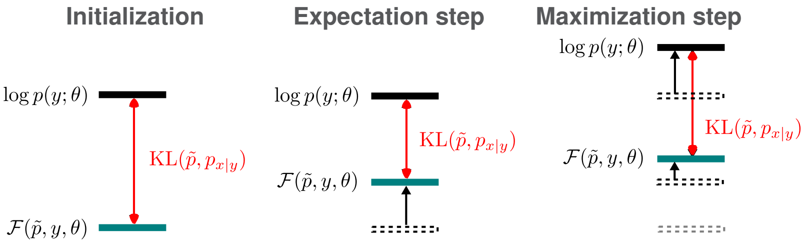

ASL JDE: VEM algorithm

[Frau-Pascual et al, 2015b]

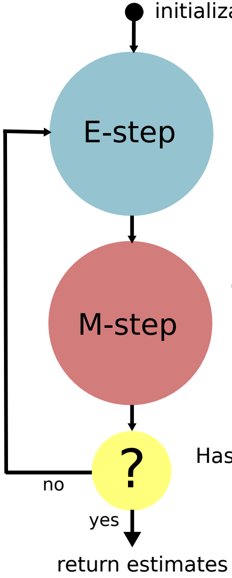

compute probability distributions

$\widetilde{p}_{a_j}(\boldsymbol{a}_j)$ $\widetilde{p}_{c_j}(\boldsymbol{c}_j)$ $\widetilde{p}_{q^m}(\boldsymbol{q}^m)$

$\widetilde{p}_h(\boldsymbol{h})$ $\widetilde{p}_g(\boldsymbol{g})$

compute parameters

$$\boldsymbol{\theta} = \{\boldsymbol{\mu}, \boldsymbol{v}, \boldsymbol{\eta}, \boldsymbol{\rho}, v_h, v_g, \beta, \boldsymbol{\ell}_j, \alpha_j, v_{b_j}\}$$

Has free energy stabilized?

$\Delta\mathcal{F}(\tilde{p}, y, \boldsymbol{\theta}) < 10^{-5}$?

ASL JDE: MCMC vs VEM solutions

[Frau-Pascual et al, 2015c]

On simulated data:

(a) Error response functions (RFs)

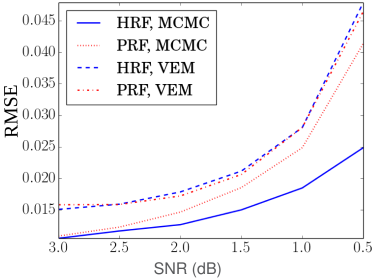

(b) Error amplitudes (RLs)

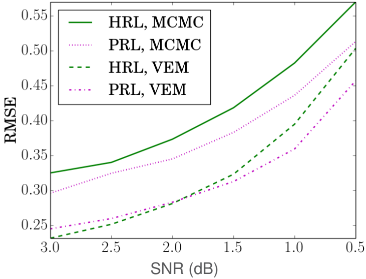

Parcel of ~ 200 voxels, real data:

MCMC (python + C)	3000 iterations	5 min
VEM (python)	60 iterations	< 1 min

VEM provides similar results with much **lower computational load**

Outline

Validation on the HEROES dataset

Data

- BOLD data
- Functional ASL data: pulsed ASL [Luh et al., 1999]
- Perfusion baseline ASL
- CBF quantification data: B1 Mapping and T1 PSSFP with angles $20°$ and $5°$.

Paradigm: motor, auditory and visual tasks.

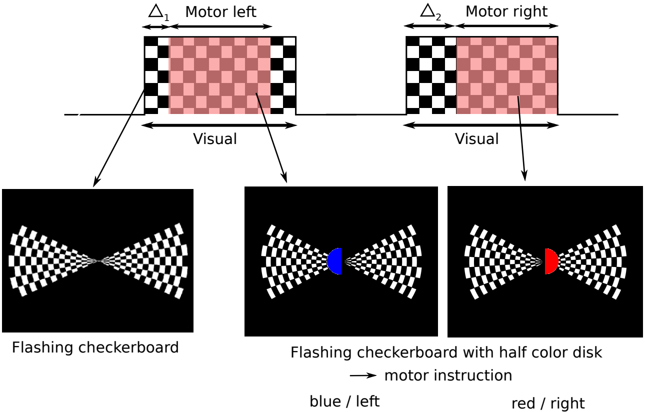

HEROES: BOLD data

Comparison of group-level results

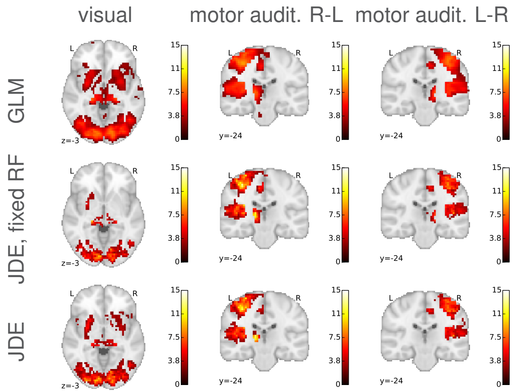

HRF estimation makes JDE find more spread activations.

JDE finds higher activation values than GLM in BOLD.

HEROES: ASL data

Comparison of group-level results

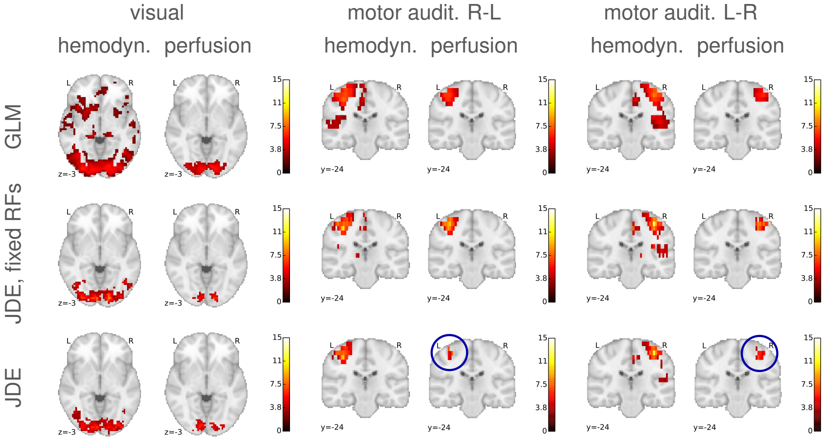

The estimation of HRF and PRF responses changes activation detection: motor cortex activation smaller.

HEROES: the smoothing effect

Impact of smoothing in the analysis

Smooth data is usually used in GLM to reduce noise and inter-subject variability. In JDE, we model the smoothing with a MRF.

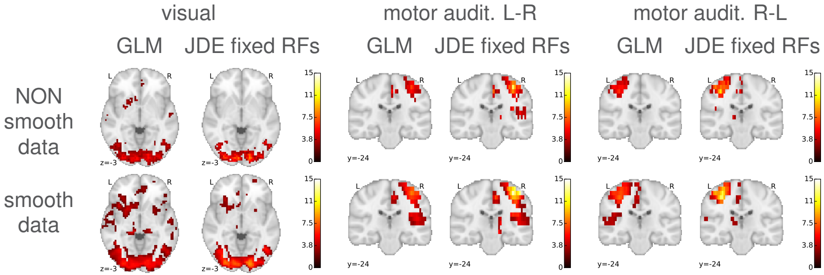

JDE (multivariate) finds more significant activation than GLM (univariate) using smooth and non-smooth data.

HEROES: the smoothing effect

Impact of smoothing in the analysis

Smooth data is usually used in GLM to reduce noise and inter-subject variability. In JDE, we model the smoothing with a MRF.

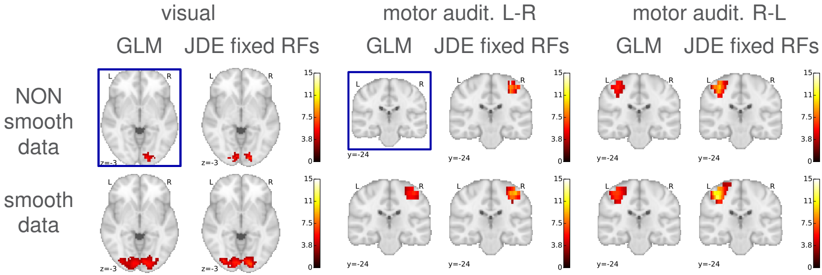

JDE (multivariate) finds more significant activation than GLM (univariate) using smooth and non-smooth data.

HEROES: BOLD vs ASL

Group level maps of BOLD, and hemodynamic and perfusion components of ASL

(a) GLM (fixed HRF and PRF responses)

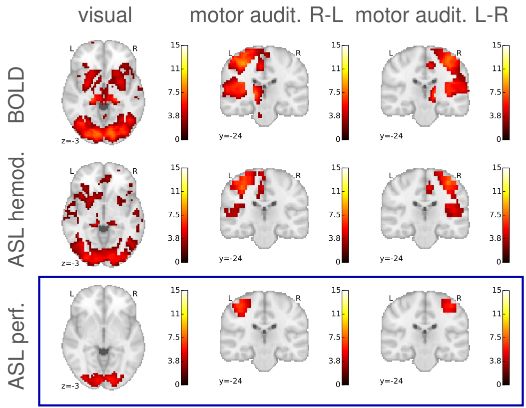

More localized activation of the perfusion ASL component.

HEROES: BOLD vs ASL

Group level maps of BOLD, and hemodynamic and perfusion components of ASL

(b) JDE with fixed HRF and PRF responses

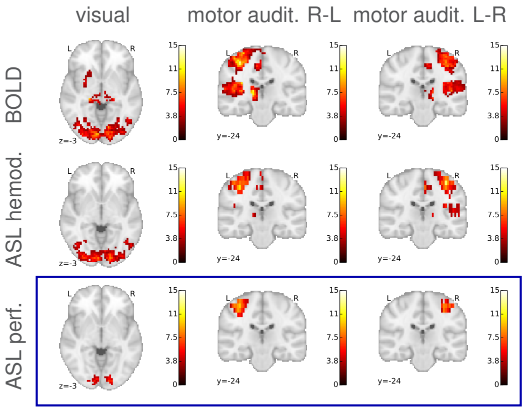

More localized activation of the perfusion ASL component.

HEROES: HRF and PRF estimation

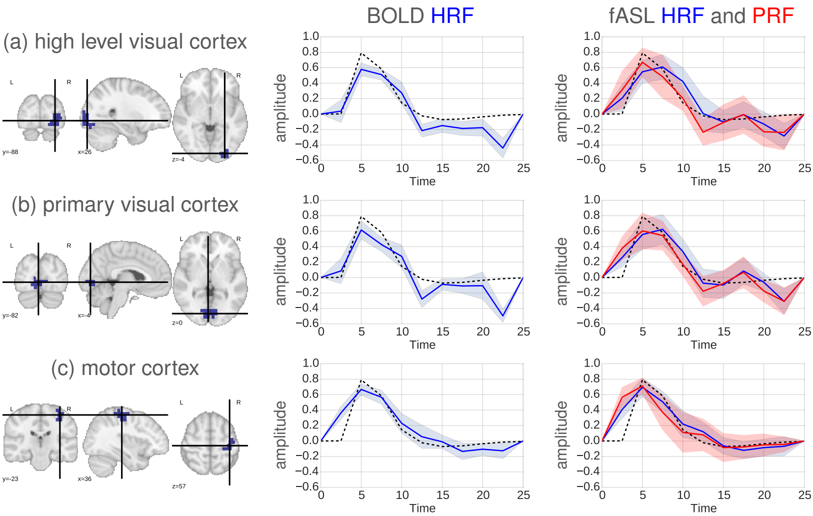

HRFs are similar in BOLD and ASL. Responses are similar between motor regions (right-left, sessions) and visual regions (right-left, sessions, V1-high visual).

HEROES: CBF quantification

[Alsop et al., 2015] states that, as a general rule, gray matter CBF values from $40 - 100$ mL/100g/min can be normal.

Basal gray matter CBF for all HEROES subjects

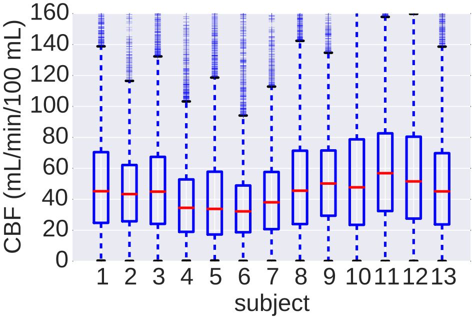

Validation on the HEROES dataset: summary

- JDE finds higher activation values than GLM in BOLD and ASL.
- HRF means are similar in BOLD and ASL, and are coherently similar in close regions.
- HRF/PRF estimation changes activation detection
  - In BOLD, we find more activated regions.
  - In ASL, some activated regions are smaller.
- Perfusion component activation more localized than BOLD.

Outline

Conclusions

This thesis has been centered around the development of tools for the neuroscientific community to analyse functional MRI.

- Introduction of physiological priors in a Bayesian framework is possible and improves estimation.
- Using the correct setting in the physiological prior improves convergence.
- VEM solution for ASL analysis is much faster and is a good approximation.
- Potential use of this tool and data modality through real data analysis compared to classical models.

Perspectives

Short term:

- Investigation of other constraints in the estimation of the perfusion response
- Adaptative physiological prior in "Bayesian" modelling, in the spirit of [Mesejo et al, 2016]
- Introduction of basal perfusion as *a priori* knowledge in JDE: change current $\alpha_j \sim \mathcal{N}(0, v_\alpha)$ to $\alpha_j \sim \mathcal{N}(\alpha_{basal,j}, v_\alpha)$.

Perspectives

Short term:

- Investigation of other constraints in the estimation of the perfusion response
- Adaptative physiological prior in “Bayesian” modelling, in the spirit of [Mesejo et al, 2016]
- Introduction of basal perfusion as *a priori* knowledge in JDE: change current $\alpha_j \sim \mathcal{N}(0, v_\alpha)$ to $\alpha_j \sim \mathcal{N}(\alpha_{basal,j}, v_\alpha)$.

Long term:

- Combination of BOLD and ASL analysis (eg. hierarchical model)
- Application to clinical research:
  - Comparison of pathological and non-pathological
  - Monitoring the evolution of a disease

Outcomes

Publication list

- A. Frau-Pascual, T. Vincent, F. Forbes, and P. Ciuciu. *"Hemodynamically informed parcellation of cerebral fMRI data"*. ICASSP 2014, pages 2079–2083.
- A. Frau-Pascual, T. Vincent, J. Sloboda, P. Ciuciu, and F. Forbes. *"Physiologically informed Bayesian analysis of ASL fMRI data"*. BAMBI 2014, pages 37–48.
- A. Frau-Pascual, F. Forbes, and P. Ciuciu. *"Variational physiologically informed solution to hemodynamic and perfusion response estimation from ASL fMRI data"*. PRNI Workshop 2015, pages 57–60.
- F. Forbes, A. Frau-Pascual, P. Ciuciu. *"Méthode d'approximation variationnelle pour l'analyse de données d'IRM fonctionnelle acquises par Arterial Spin Labelling"*. GRETSI, Sep 2015, Lyon, France.
- A. Frau-Pascual, F. Forbes, and P. Ciuciu. *"Comparison of stochastic and variational solutions to ASL fMRI data analysis"*. MICCAI 2015 , pages 85–92.
- A. Frau-Pascual, F. Forbes, and P. Ciuciu. *"Physiological models comparison for the analysis of ASL fMRI data"*. ISBI 2015 , pages 1348–1351.

PyHRF code, together with the PyHRF team (GIN+Inria+Neurospin)

- BOLD VEM multiple-session extension
- Physiologically informed ASL MCMC
- Physiologically informed ASL VEM

Thank you

Questions

Physiological prior in JDE: options considered

- Stochastic Ω constraint (1-step or 2-step)

$$\boldsymbol{h} \sim \mathcal{N}(0, v_h \boldsymbol{\Sigma}_h)$$
$$\boldsymbol{g}|\boldsymbol{h} \sim \mathcal{N}(\boldsymbol{\Omega h}, v_g \boldsymbol{\Sigma}_g)$$

- Deterministic Ω constraint

$$\boldsymbol{h} \sim \mathcal{N}(0, v_h \boldsymbol{\Sigma}_h)$$
$$\boldsymbol{g} = \boldsymbol{\Omega h}$$

- Hierarchical model

$$\boldsymbol{h}_t \sim \mathcal{N}(\boldsymbol{h}_{can}, v_{h_t} \boldsymbol{\Sigma}_{h_t}) : \quad \text{true HRF}$$
$$\boldsymbol{h}|\boldsymbol{h}_t \sim \mathcal{N}(\boldsymbol{h}_t, v_h \boldsymbol{\Sigma}_h) : \quad \text{noisy HRF}$$
$$\boldsymbol{g}|\boldsymbol{h}_t \sim \mathcal{N}(\boldsymbol{\Omega h}_t, v_g \boldsymbol{\Sigma}_g) : \quad \text{PRF}$$

- Balloon model

$$\boldsymbol{h} \sim \mathcal{N}(\boldsymbol{h}_{balloon}, v_h \boldsymbol{\Sigma}_h)$$
$$\boldsymbol{g} \sim \mathcal{N}(\boldsymbol{g}_{balloon}, v_g \boldsymbol{\Sigma}_g)$$

Thanks to everyone!